

The manuscript has been submitted for publication in *ADVANCES IN ATMOSPHERIC SCIENCES*.

Please note that, despite having undergone peer-review, the manuscript has yet to be formally accepted for publication. Subsequent versions of this manuscript may have slightly different content.

If accepted, the final version of this manuscript will be available via the "Peer-reviewed Publication DOI" link on the right-hand side of this webpage. Please feel free to contact the author, I welcome feedback.

1 **Reducing uncertainties in climate projections with emergent**
2 **constraints: Concepts, Examples and Prospects**

3 **Florent Brient¹**

4 ¹CNRM, Université de Toulouse, Météo-France, CNRS, Toulouse France

5 6958 words

Corresponding author: Florent Brient, florent.brient@gmail.com

6 Abstract

7 Models disagree on a significant number of responses to climate change, such as climate feedback,
8 regional changes, or the strength of equilibrium climate sensitivity. Emergent constraints aim to
9 reduce these uncertainties by finding links between the inter-model spread in a observable predictor
10 and climate projections. In this paper, I recall the concepts underlying this framework with an em-
11 phasis on the statistical inference used for narrowing uncertainties, and review emergent constraints
12 found in the last two decades. I investigate potential links between highlighted predictors, especially
13 those targeting uncertainty reductions in climate sensitivity, cloud feedback, and changes of the
14 hydrological cycle. I also show that the disagreement across emergent constraints do not robustly
15 narrow the spread in climate sensitivity. This calls for weighting the realism of emergent constraints
16 by quantifying the level of physical understanding explaining the relationship. This would also
17 permit more efficient model evaluation and better targeted model development. In the context of
18 the upcoming CMIP6 model intercomparison, I expect a growing number of new predictors and
19 uncertainty reductions which call for robust statistical inferences that allow cross-validation of more
20 likely estimates.

21 1 Introduction

22 For more than two centuries, steadily increasing carbon dioxide concentrations in the atmosphere
23 have been warming the Earth. Today it is 0.8°C warmer than in the preindustrial period in the
24 middle of the 19th century [Morice *et al.*, 2012]. Global climate models (GCMs) project how
25 this global warming will continue given the expected continuous increase in human-made carbon
26 dioxide emissions. While models agree on the sign of a number of climate change signals, they often
27 disagree on their amplitude [Flato *et al.*, 2013]. A well-known example is the equilibrium climate
28 sensitivity (ECS), i.e. the equilibrium global-mean surface temperature increase resulting from a
29 sustained doubling of carbon dioxide concentrations [Gregory *et al.*, 2004]. For decades, models
30 have exhibited widely differing climate sensitivities, yet with a range remaining roughly between 2
31 and 5°C [Charney *et al.*, 1979; Bony *et al.*, 2013]. To correctly predict how much the Earth will
32 warm, one must know at least (1) how carbon dioxide concentration will evolve [Stocker *et al.*, 2013],
33 and (2) the correct value of climate sensitivity.

34 A doubling of the carbon dioxide concentration would warm the Earth by $1.2 \pm 0.1^{\circ}\text{C}$ [Dufresne
35 and Bony, 2008]. However, this warming induces changes that can amplify or dampen the initial
36 temperature response through feedback processes [Bony *et al.*, 2006]. For example, the CO_2 -induced
37 global warming allows the atmosphere to hold more water vapor. This acts as a positive feedback on

the surface warming, because water vapor itself is a powerful greenhouse gas that, like CO₂, absorbs and re-emits long-wave radiation back to the surface. This is somewhat compensated by the negative temperature lapse rate feedback that allows more outgoing long wave emission to be emitted out of the atmosphere. The initial warming also reduces the surface albedo by melting snow and sea-ice, which also constitutes a positive feedback because snow and ice are effective reflectors of sunlight. Models agree on the sign and approximately the amplitude of these two feedback processes [Ceppi *et al.*, 2017]. The water vapor, lapse-rate, and ice-albedo feedbacks in isolation enhance the global warming due to increasing CO₂ concentrations to around +2.2°C [Dufresne and Bony, 2008]. Models disagree on the cloud response to surface warming, which is primarily why they produce a wide range of ECS values, e.g. between 2.1 and 4.7°C for the CMIP5 model intercomparison [Flato *et al.*, 2013]. Since clouds have dynamical scales in the order of tens to hundreds of meters, climate models with grid boxes of hundred of kilometers cannot explicitly resolve cloud processes. Empirically-based assumptions are thus used to relate unresolvable small-scale dynamics to properties (temperature, humidity etc.) on the models' grid scale. Those parameterizations are the heart of biases in reproducing the present-day climate and of uncertainties in climate change projections [e.g. Brient *et al.*, 2016]. This calls for new efficient process-oriented methods for understanding leading causes behind these uncertainties and for establishing better model evaluation and development.

2 Emergent constraints

2.1 Definition

Recently, a methodology called emergent constraint has been developed for reducing uncertainties in climate-change projections. This framework is based on :

1. identifying responses to climate change perturbation in which model disagree (e.g., cloud feedback)
2. relating the inter-model spread in the climate-change responses to present-day biases or short-term variations that can be observed.

This could be achieved by identifying an empirical relationship between the inter-model spread of an observable variable (hereafter named A) and the inter-model responses B to a given perturbation. The variable A is called the predictor and the variable B the predictand. Because observed measurements of the predictor A can then be used to constrain the models' responses B, the relationship between A and B is called an emergent constraint [Klein and Hall, 2015]. The variable A may represent a metric that characterize the climate system (humidity, winds,...) or may characterize natural variability

(e.g., in the seasonal cycle, or from year to year). The response B can be the global-mean response of the climate system (e.g. ECS) or a local response to perturbations (e.g. a regional climate feedback). Therefore, the goal is to find a predictor that, given its relation to a climate response, emerges as a constraint on future projections.

Once the variable A is estimated observationally, the emergent constraint can be used to assess models' realism and to eventually narrow the spread of climate change projections. As an idealized example, Figure 1 shows a randomly-generated relationship between a predictor A simulated by 29 climate models and a projection of future climate changes (in principle any climate-change response may be considered). The green distribution represents an observational measurement and its uncertainties. We see that differences in A are significantly associated with differences in B, here with a correlation coefficient of $r=0.83$. By constraining A through observations (green distribution), this example suggests that some models are more realistic and, by inference, are associated with more realistic future climate sensitivities. The degree to which the models' A deviates from the observed A can be used to derive weights for the models to compute a weighted average of the models' response B (see section 2.2.3).

2.2 Criterion and uncertainties

2.2.1 Physical understanding

An emergent constraint can be trusted if it meets certain criteria. The most important one is an understanding of physical mechanisms underlying the empirical relationship, which is the key to increase the plausibility of a proposed emergent constraint. Several methods have been recently suggested to verify the level of confidence of emergent constraints [Caldwell *et al.*, 2018; Hall *et al.*, 2019]. One of them consists in checking the reliability of an emergent constraint by developing sensitivity tests that would modify A for some models (if there is a straightforward way of manipulating A). For accurate model comparison, this would require coupled model simulations with global-mean radiative balance as performed for CMIP intercomparison. If the models' behavior after the modification deviates from that expected from the emergent constraint, the relationship may have been found by chance. A study showed that this risk is not negligible [Caldwell *et al.*, 2014], primarily because climate models are not independent but many are derived from each other [Masson and Knutti, 2011; Knutti *et al.*, 2013]. Keeping only models with enough structural differences often reduces the reliability of identified emergent constraints. The search for correlations with no obvious physical understanding could lead to such spurious results. Conversely, if those sensitivity

100 tests confirm the inter-model relationship, the credibility of assumed physical mechanisms and
101 observational constraints on climate change projections increases. Those tests could be performed
102 through a multiparameter multiphysics ensemble that would help (1) disentangle structural and
103 parametric influence on the multi-model spread in predictor A and (2) highlight underlying processes
104 explaining the empirical relationship [*Kamae et al.*, 2016].

105 **2.2.2 Observation uncertainties**

106 The second criterion is related to the correct use of observations. Uncertainties tied to the
107 observation of the predictor must be small enough so that not all models remain consistent with the
108 data. This criterion may not be satisfied if observations are available only over a short time period (as
109 is the case for the vertical structure of clouds, [e.g. *Winker et al.*, 2010]), or if the predictor is defined
110 through low-frequency variability (trends, decadal variability), or if there is a lack of consistency
111 among available datasets (as in the case for global-mean precipitation and surface fluxes, [e.g.
112 *Găinușă-Bogdan et al.*, 2015]). Finally, some *observational* constraints rely on parameterizations
113 used in climate models, e.g. reanalysis that use sub-grid assumptions for representing clouds [e.g.
114 *Dee et al.*, 2011] or data product for clouds that use sub-grid assumptions for radiative transfer
115 calculations [*Rossow and Schiffer*, 1999].

116 **2.2.3 Statistical inference**

117 Emergent constraints can allow us to narrow uncertainties and quantify more likely estimates
118 of climate projections, i.e. constrained posterior range of a prior distribution. However, not all
119 emergent constraints should be given the same trust. *Hall et al.* [2019] suggested to relate this trust
120 to the level of physical understanding associated with the emergent relationship. This means making
121 predictions only for confirmed emergent constraints.

122 Posterior estimates are influenced by the way the statistical inference has been performed.
123 However, no consensus has yet emerged for this inference. A first method for quantifying this
124 constraint is to directly use uncertainties underlying the observational predictor and project it onto the
125 vertical axis using the emergent constraint relationship. This method takes into account uncertainties
126 in both observations and the estimated regression model, through bootstrapping samples for instance
127 [*Huber et al.*, 2011]. Most studies use this straightforward framework. In our idealized example,
128 this would give a posterior estimate of 4.0 ± 0.5 (narrower than the raw estimate as seen on Figure 1).
129 However, several problems with this kind of inference might be highlighted:

- 130 • Most fundamentally, the inference generally revolves around assuming that there exists a
131 linear relationship, and estimating parameters in the linear relationship from climate models.
132 But it is not clear that such a linear relationship does in fact exist, and estimating parameters
133 in it is strongly influenced by models that are inconsistent with the observations (extreme
134 values). In other words, the analysis neglects structural uncertainty about the adequacy of the
135 assumed linear model, and the parameter uncertainty the analysis does take into account is
136 strongly reduced by models that are "bad" by this model-data mismatch metric. Outliers thus
137 strongly influence the result. However, the influence of models consistent with the data but
138 off the regression line is diminished. Given that there is no strong a priori knowledge about
139 any linear relationship – this is why it is an "emergent" constraint – it seems inadvisable to
140 make one's statistical inference strongly dependent on models that are not consistent with the
141 data at hand.
- 142 • Often analysis parameters are chosen so as to give strong correlations between the response
143 of models to perturbations and the predictor. This introduces selection bias in the estimation
144 of the regression lines. This leads to underestimation of uncertainties in parameters, such
145 as the slope of the regression line, which propagates into underestimated uncertainties in the
146 inferred estimate.
- 147 • When regression parameters are estimated by least squares, the observable on the horizontal
148 axis is treated as being a known predictor, rather than as being affected by error (e.g., from
149 sampling variability). This likewise leads to underestimation of uncertainties in regression
150 parameters. This problem can be mitigated by using errors-in-variables methods.

151 A second method consists of estimating a posterior distribution by weighting each model's
152 response by the likelihood of the model given the observations of the predictor. This can be
153 accomplished by a Bayesian weighting method [e.g. *Hargreaves et al.*, 2012] or through information
154 theory [e.g. *Brient and Schneider*, 2016], such as the Kullback-Leibler divergence or relative entropy
155 [*Burnham and Anderson*, 2010]. This method does not use the linear regression for estimating
156 the posterior distribution and therefore favor realistic models and deemphasize outliers inconsistent
157 with observations. The Kullback-Leibler divergence applied to our idealized example (assuming an
158 identical standard deviation between observation and each model) suggests an estimate of 3.4 ± 0.7
159 (Figure 1).

160 This more justifiable inference still suffers from several shortcomings. For example, it suffers
161 from selection bias, and it treats the model ensemble as a random sample (which it is not). It

162 also only weights models, suggesting that climate projections far outside the range of what current
163 models produce will always come out as being very unlikely. Given uncertainties underlying each
164 method, posterior estimates should thus be quantified using different methods (as previously done in
165 *Hargreaves et al. [2012]* for instance) and methods should be significantly described.

166 Figure 2 provides a tangible example for explaining the importance of statistical inference.
167 It shows the relation in 29 current climate models between ECS and the strength with which the
168 reflection of sunlight in tropical low-cloud regions covaries with surface temperature [*Brient and*
169 *Schneider, 2016*]. That is, the horizontal axis shows the percentage change in the reflection of
170 sunlight per degree surface warming, for deseasonalized natural variations. It is clear that there is
171 a strong correlation (correlation coefficient about -0.7) between ECS on the vertical axis and the
172 natural fluctuations on the horizontal axis (an example of an empirical fluctuation-dissipation relation
173 in the models). The green line on the horizontal axis indicates the probability density function (PDF)
174 of the observed natural fluctuations. What many previous emergent-constraint studies have done is
175 to take such a band of observations and project it onto the vertical ECS axis using the estimated
176 regression line between ECS and the natural fluctuations, taking into account uncertainties in the
177 estimated regression model. If we do this with the data here, we obtain an ECS that likely lies within
178 the blue band: between 3.1 and 4.2 K, with a most likely value of 3.6 K. Simply looking at the scatter
179 of the 29 models in this plot indicates that this uncertainty band is too narrow. For example, model
180 7 is consistent with the observations, but has a much lower ECS of 2.6 K. The regression analysis
181 would imply that the probability of an ECS this low or lower is less than 4%. Yet this is one of
182 29 models, and one of relatively few (around 9) that are likely consistent with the data. Obviously,
183 the probability of an ECS this low is much larger than what the regression analysis implies. As
184 explained before, these flaws could be reduced by weighting ECS by the likelihood of the model
185 given the observations. Models such as numbers 2 and 3, which are inconsistent with observations,
186 would receive essentially zero weight (unlike in the regression-based analysis, they do not influence
187 the final result). No linear relationship is assumed or implied, so models such as 7 receive a large
188 weight because they are consistent with the data, although they lie far from any regression line. The
189 resulting posterior PDF for ECS is shown by the orange line in Figure 1b. The most likely ECS
190 value according to this analysis is 4.0 K. It is shifted upward relative to the regression estimate,
191 toward the values in the cluster of models (around numbers 25 and 26) with relatively high ECS
192 that are consistent with the observations. The likely ECS range stretches from 2.9 to 4.5 K. This
193 is perhaps a disappointingly wide range. It is 50 % wider than what the analysis based on linear

194 regressions suggests, and it is not much narrower than what simple-minded equal weighting of raw
195 climate models gives (gray line in Figure 1b). But it is a much more statistically defensible range.

196 In order to generalize the sensitivity of inferred estimates to the statistical methodology, I
197 generate 10^4 random emergent relationships and plot statistics of inferences (mode, confidence
198 intervals) as a function of averaged correlation coefficients. Figure 3 shows that averaged modes and
199 confidence intervals are consistent between the two inference methods for this set of relationships.
200 However, the variance of inferred best estimates (modes) using the weighting method is larger than
201 the one using the inference method. This is in agreement with results obtained from the tangible
202 example from *Brient and Schneider* [2016], which show different most likely values. Therefore, this
203 suggests the best estimate is significantly influenced by the way statistical inference is performed.

204 Finally, uncertainties underlying these estimates may be influenced by the level of structural
205 similarity between climate models. Indeed, adding models with only weak structural differences
206 (e.g. model version with different resolution, interactive chemistry) can artificially strengthen the
207 correlation coefficient of the empirical relationship and the inferred best estimate [*Sanderson et al.*,
208 2015]. This coefficient is usually the first criterion that quantify the statistical credibility of an
209 emergent constraint, i.e. the larger the correlation coefficient, the more trustworthy the regression-
210 based inference will be. However, it remains unknown what level of statistical significance justifies
211 an emergent constraint and whether these correlation best characterize their credibility.

212 **3 Pioneering studies**

213 In the following sections, I aim to describe emergent constraints that have been highlighted
214 within the last two decades. Table 1 summarize them, along with prior and posterior estimates of
215 the models' predictand. Mean and uncertainties (one standard deviation) are based on the inference
216 provided in the reference if available, or roughly derived through their empirical relationship and
217 observational uncertainties otherwise (for qualitative assessment).

218 In the late 1990s, signs of climate feedback started to be constrained from climate models and
219 observations [e.g. *Hall and Manabe*, 1999]. Usually analyzing one unique model, these studies
220 improved our understanding of physical mechanisms driving climate feedback. However, the lack
221 of inter-model comparisons in these studies did not allow quantifying the relative importance of
222 feedbacks in driving uncertainties in climate change projections. Model intercomparisons during
223 this period identified the cloud response to global warming as being the key contributor of inter-model

224 spread in climate projections [*Cess et al.*, 1990, 1996]. Both types of studies thus pave the way toward
225 process-oriented investigation for understanding inter-model differences in climate projections.

226 To my knowledge, the first attempt at introducing the concept of emergent constraint was
227 made by *Allen and Ingram* [2002]. The authors tried to constrain the spread in global-mean future
228 precipitation change simulated by the set of climate models participating in the CMIP2 model
229 intercomparison project [*Meehl et al.*, 2000] through observable temperature variability and a simple
230 energetic framework. Despite the inability to robustly narrow future precipitation changes, they
231 introduced the concepts that establish emergent constraints: the need for physical understanding and
232 the ability of observations to constrain the model predictor.

233 An early application of emergent constraints concerns the snow-albedo feedback. *Hall and*
234 *Qu* [2006] showed that differences among models in seasonal northern hemisphere surface albedo
235 changes are well correlated with global-warming albedo changes in CMIP3 models. The three main
236 criteria for a robust emergent constraint are satisfied: the physical mechanisms are well understood,
237 the statistical relationship between the quantities of interest is strong, and uncertainties in the observed
238 variations are weak, allowing the authors to constrain the northern hemisphere snow-albedo feedback
239 under global warming. Despite this successful application, the generation of models that followed
240 (CMIP5) continued to exhibit a large spread in seasonal variability of snow-albedo changes [*Qu and*
241 *Hall*, 2014]. This could be narrowed through targeted process-oriented model development based
242 on the evaluation of snow and vegetation parameterizations [*Thackeray et al.*, 2018]. Yet this study
243 can be seen as the first confirmed emergent constraint [*Klein and Hall*, 2015; *Hall et al.*, 2019].

244 The success of the Hall and Qu study led a number of studies to seek emergent constraints
245 able to narrow climate-change responses. In the following sections, I review these studies which
246 aim to constrain equilibrium climate sensitivity, cloud feedback, or various changes in Earth system
247 components, such as the hydrological cycle or the carbon cycle.

248 **4 Model biases and equilibrium climate sensitivity**

249 Uncertainties in ECS usually scale with uncertainties in regional climate changes [*Seneviratne*
250 *et al.*, 2016]. So constraining ECS would help estimating regional responses to climate change,
251 which matter the most for impact studies and risk assessment. Therefore, a majority of emergent
252 constraints prioritize providing a better range for ECS, as shown on table 1.

253 The main predictors used to constrain the spread in ECS consist of observable climatological
254 characteristics of the current climate. The first study using this approach was *Volodin* [2008], which

255 found that CMIP3 models with large ECS are more likely to exhibit (1) large differences in cloud
256 cover between the tropics and the extra-tropics and (2) low tropical relative humidity.

257 The first estimate suggested by *Volodin* [2008] uses a cloud climatology from geostationary
258 satellites to derive a more likely ECS range of 3.6 ± 0.3 K. This range is slightly higher than the
259 multi-model average, with a reduced variance (Table 1). However this study does not address the
260 physical understanding of links between clouds, moisture, and climate feedbacks, which reduce the
261 credibility of this estimate. A more recent study, *Siler et al.* [2018], provides a physical interpretation
262 underlying this cloud constraint. They hypothesize that the need for a global-mean radiative balance
263 (through model tuning) forces a link between warm and cold regions, i.e. models having less clouds
264 in the tropical area will very likely simulate more extratropical clouds in the current climate. Given
265 that the global warming will expand tropical warm regions at the expense of extratropical cold
266 regions, these models will increase the spatial coverage of areas with weak cloudiness relative to the
267 multi-model mean, leading to more positive low-cloud feedback and high climate sensitivity. Using
268 observations for characterizing the spatial coverage of cloud albedo, *Siler et al.* [2018] find a best
269 ECS estimate of 3.7 ± 1.3 K, in agreement with *Volodin* [2008].

270 The second estimate suggested by *Volodin* [2008] is related to relative humidity and uses re-
271 analysis outputs to provide a more likely ECS range of 3.4 ± 0.3 K. In CMIP3, models with largest
272 zonal-mean relative humidity over the subtropical free troposphere are those with the lowest climate
273 sensitivity. Given that models generally overestimate this predictor, this suggests the highest ECS
274 values are more realistic. This is in agreement with *Fasullo and Trenberth* [2012], which found
275 the same relationship and a best ECS estimate of around 4 K (Table 1). This emergent relationship
276 is somewhat explained by the broadening of the tropical dry zones with global warming, which
277 imply a drying of the subsiding branches. Thus, the drier the free troposphere in the current climate
278 the stronger the boundary-layer drying and cloud feedback with global warming. This mechanism
279 may also explain the positive low-cloud feedback in climate models, e.g. the IPSL-CM5A model
280 [*Brient and Bony*, 2013]. Conversely, *Volodin* [2008] hypothesized that the relationship is related to
281 the role of relative humidity in convective parameterization. These different physical interpretations
282 suggest that emergent constraints arise from inter-model differences in structural (local) uncertainties,
283 (remote) biases in large-scale dynamics, and the interactions between them.

284 This dichotomy is addressed by *Sherwood et al.* [2014]. They quantify the low-tropospheric
285 convective mixing through the sum of two metrics : an index related to small-scale mixing and an
286 index linked to large-scale mixing. The former aims to represent errors in parameterized processes

287 such as shallow convection, turbulence, or precipitation. The latter quantifies model errors in
288 reproducing the tropical dynamical circulation, which can also be affected by parameterizations of
289 deeper convection remotely affecting low-clouds. The CMIP3 and CMIP5 inter-model spread of this
290 predictor is well correlated to uncertainties in ECS. Observations (here reanalysis) suggest that most
291 models underestimate this large-scale mixing, indicating a most likely ECS value larger than 3 K
292 (Table 1). The level of confidence in this estimate is related to the trust one gives to the link between
293 the low-tropospheric characteristics these indices aim to quantify and the low-cloud feedback, which
294 primarily controls the intermodel spread in ECS. The observational constraint should also be viewed
295 with caution since it is based on re-analysis data and hence is influenced by parameterizations.

296 The mixing index suggested by *Sherwood et al.* [2014] highlights that errors in representing the
297 coupling between low-clouds and tropical dynamics explain a significant part of the spread in ECS, in
298 agreement with *Volodin* [2008] and *Fasullo and Trenberth* [2012]. This was confirmed by follow-up
299 studies that suggested significant correlations between ECS and indexes of the tropical dynamics,
300 such as the strength of the double-ITCZ bias [*Tian*, 2015] or the strength of the Hadley circulation
301 [*Su et al.*, 2014]. Both show that models better representing the tropical large-scale dynamics are
302 those with the highest climate sensitivities (≈ 4 K). However the lack of robust physical mechanisms
303 explaining these emergent constraints reduces the trustfulness of these inferences, but it also prompts
304 for better theoretical understanding of links between cloud and circulation. This question can be
305 investigated by analyzing the driving influence of clouds on the energetic balance of the atmosphere
306 for explaining large-scale dynamical biases, whether clouds are located in the southern hemisphere
307 [*Hwang and Frierson*, 2013] or in the tropical subsiding regions [*Adam et al.*, 2016, 2017]. Together
308 these studies suggest hidden relationships between low clouds, circulation, and climate sensitivity,
309 which remain to be clarified.

310 The spread in ECS can also be constrained through the past variability in global-mean tempera-
311 ture, as suggested by *Cox et al.* [2018]. Observations suggests that a majority of models overestimate
312 temperature variations and year-to-year autocorrelation, providing a most likely posterior ECS es-
313 timate of 2.8 ± 0.6 K (Table 1). Contrary to most of emergent constraints, this study thus suggests
314 a relative low best estimate for climate sensitivity. The absence of links between the mathematical
315 framework used to build the predictor and clouds might reduce the confidence in this estimate.
316 However, low-frequency natural variability of tropical temperature seems partly related to cloud
317 variability [e.g. *Zhou et al.*, 2016], so it can not be excluded that all these emergent constraints are
318 related to each other. Process-oriented cross-metric analysis would be necessary to support this
319 hypothesis [e.g. *Wagman and Jackson*, 2018].

5 Cloud feedback

The spread of climate sensitivity is significantly related to the spread in cloud feedback, and mostly to uncertainties in low-cloud responses. It therefore appears obvious that constraining how low clouds respond to global warming would very likely reduce the spread of climate sensitivity among models, and that many emergent constraints on ECS can be understood as encoding properties of shortwave low-cloud feedbacks [Qu *et al.*, 2018]. Conversely, emergent constraints that are only indirectly related to clouds should be viewed with caution.

A number of studies have highlighted relationships between low-cloud amount changes under global warming and modeled variations of low clouds with changes in specific meteorological conditions, such as surface temperature, inversion strength, subsidence [Qu *et al.*, 2013, 2015; Myers and Norris, 2013, 2015; Brient and Schneider, 2016]. These studies suggest two robust low-cloud feedbacks: a decrease in low-cloud amount with surface warming (related to increasing boundary-layer ventilation) and an increase of low-cloud amount with inversion strengthening (related to a reduced cloud-top entrainment of dry air). Models show that the former feedback mostly dominates the latter under a global warming, and that the more realistic models exhibit larger low-cloud feedback [Qu *et al.*, 2013, 2015; Brient and Schneider, 2016]. The convergence of studies using different methodologies and different observations increases our confidence that low-cloud amount feedback more likely lie in the upper range of simulated estimates.

Given that the strength of low-cloud amount feedback strongly correlates with ECS, temporal variations in low-cloud albedo appears as a credible metric for constraining ECS. Observations suggests most likely ECS estimates around 4 K, roughly identical for different temporal frequencies of cloud variations [Zhai *et al.*, 2015; Brient and Schneider, 2016]. Despite this robustness, these conclusions are sensitive to the short time period (around a decade) over which observations provide accurate enough characteristics of low-clouds. Low-cloud short-term variations might only partly reflect long-term feedback [Zhou *et al.*, 2015], likely because of slow evolving spatial pattern of surface temperature that delay inversion changes and cloud feedback in subsiding regions [Ceppi and Gregory, 2017; Andrews *et al.*, 2018].

Although low-cloud amount feedback is the main driver of uncertainties in climate sensitivity, other cloud responses contribute to the spread as well. One of them is the low-cloud optical feedback, which is defined by the radiative influence of changes in optical properties given unchanged cloud amount and altitude. Gordon and Klein [2014] show that the natural variability of mid-latitude cloud optical depth with temperature is well correlated with its changes with global warming.

352 This relationship stems from fundamental thermodynamics, i.e. the increase in water content with
353 warming [Betts and Harshvardhan, 1987], and microphysical changes, i.e. the relative increase of
354 liquid content relative to ice within clouds [Mitchell *et al.*, 1989]. This supports a robust negative
355 cloud optical feedback with warming. Observations suggest that models are usually biased high, thus
356 overestimating the negative mid-latitude low-cloud optical feedback. A misrepresentation of mixed-
357 phase processes within these extratropical clouds may explain this bias [McCoy *et al.*, 2015], which
358 has been pinpointed as being a key driver of differences in cloud feedback and climate sensitivity
359 estimates [Tan *et al.*, 2016].

360 The cloud altitude response to global warming may also amplify the original warming, and
361 models continue to disagree on the strength of this feedback [Zelinka *et al.*, 2013]. Physical
362 mechanisms of high cloud elevation with warming are well understood [Hartmann and Larson, 2002],
363 making high-cloud altitude feedback very likely positive. Yet it remains unknown to what extent the
364 high-cloud amount and the high-cloud optical depth change with warming. These changes are related
365 to upper-tropospheric divergence and microphysics, which need to be constrained individually. Some
366 studies suggest a decreasing high-cloud amount due to more efficient large-scale organization with
367 warming [e.g. Bony *et al.*, 2016], which point the way towards mechanistic emergent constraints on
368 high-cloud feedback.

369 Better constraining cloud feedback will therefore very likely lead to better constraints on the
370 equilibrium climate sensitivity. This target should be addressed through process-based understanding
371 of individual cloud changes, such as how the relative coverage of tropical low clouds evolves, how
372 high cloud fraction change as they move upward, or to what extent small-scale microphysical changes
373 perturb the climate system. Merging realistic estimates of these feedbacks would give a step forward
374 for accurately constraining the equilibrium climate sensitivity.

375 **6 Constraining Climate Changes**

376 In the last decade, the concept of emergent constraints has begun to be widely applied in different
377 branches of climate science that allowed constraining uncertain responses of the Earth system, such
378 as the hydrological cycle, the carbon cycle, or various regional changes.

379 **6.1 The hydrological cycle**

380 Uncertainties in the response of precipitation to global warming are important and remain to be
381 narrowed. Increasing the confidence in precipitation changes would provide important benefits for

382 regional climate projections and risk assessment [*Christensen et al.*, 2013]. Links between natural
383 variability of extreme precipitation and temperature offer possible observational constraints for
384 changes in climate extremes, especially because the underlying physical mechanisms are relatively
385 well understood [*O’Gorman and Schneider*, 2008]. These constraints usually suggest a strong
386 intensification of heavy rainfall with warming [*O’Gorman*, 2012; *Borodina et al.*, 2017]. Changes
387 in the hydrological cycle can partly be attributed to changes in the clear-sky shortwave absorption,
388 which is related to models’ radiative transfer parameterizations [*DeAngelis et al.*, 2015]. That
389 emphasis on processes that explain inter-model difference in the predictor might lead to targeted
390 model development for narrowing climate projections.

391 **6.2 The carbon cycle**

392 A second topic that has also received great emphasis is the sensitivity of the carbon cycle to
393 climate change. *Cox et al.* [2013] found a robust relationship that links interannual co-variations
394 between tropical temperature and carbon release into the atmosphere (the predictor) and the weak-
395 ening in carbon storage under global warming. Observations highlight that most climate models
396 overestimate the present-day sensitivity of land CO₂ changes, suggesting a too strong weakening of
397 the CO₂ tropical land storage with climate change (Table 1). This constraint has been confirmed
398 by following analysis [*Wang et al.*, 2014; *Wenzel et al.*, 2014]. Additional studies have aimed to
399 constrain other aspects of the climate-carbon cycle feedback, such as the land photosynthesis [*Wenzel*
400 *et al.*, 2016], sinks and sources of carbon dioxide [*Hoffman et al.*, 2014; *Winkler et al.*, 2019], and
401 the tropical ocean primary production [*Kwiatkowski et al.*, 2017].

402 **6.3 Geoengineering**

403 Constraining uncertainties in geoengineering simulations has also been addressed. Inter-model
404 differences in the climate response to an artificial increase of sulfate concentrations are correlated to
405 inter-model differences in the simulated cooling by past volcanic eruptions [*Plazzotta et al.*, 2018].
406 Physical assumptions underlying this relationship consists in assuming that volcanic eruptions can be
407 understood as an analogue of solar radiation management [*Trenberth and Dai*, 2007]. Observations
408 from satellites suggest that models overestimate the cooling by volcanic eruptions, thus overestimating
409 the potential cooling effect by an addition of aerosols in the stratosphere.

6.4 Regional climate changes

While most emergent constraints focus on global scales, several aim to better understand and constrain regional climate changes. So far these studies mostly focus on extratropical climate responses, as was the case for the pioneering work of *Hall and Qu* [2006]. Attempts in constraining changes of extreme temperature have recently showed that models slightly overestimate the increasing frequency of heat extremes with global warming in Europe and North America [*Donat et al.*, 2018], in relation with a too strong soil drying [*Douville and Plazzotta*, 2017]. Changes in the extratropical circulation have also been studied. Models show a robust poleward shift of the South Hemisphere jet with global warming, and are uncertain about the sign of the North Hemisphere jet shift. Emergent constraints and statistical inference suggest that models overestimate the southern hemispheric poleward shift [*Kidston and Gerber*, 2010; *Simpson and Polvani*, 2016] and predict that the northern hemisphere jet will likely move poleward [*Gao et al.*, 2016]. Finally, a number of studies aim to constrain changes over the Arctic region. They show that a majority of models delays the year when summertime sea-ice cover would likely disappear [*Boé et al.*, 2009; *Massonnet et al.*, 2012] and slightly overestimates the strength of the polar amplification [*Bracegirdle and Stephenson*, 2013].

Regional emergent constraints remain rare, which reduce the ability to compare metrics and observations to one another. Results are thus not robust yet, and should be viewed with caution. However, knowing the large uncertainties underlying regional climate projections and the advantages local populations will get from better model projections [*Christensen et al.*, 2013], I expect to see numerous new emergent constraints aimed to narrow uncertainties in regional climate changes in the near future. Nevertheless, this should be addressed through rigorous physical understanding given the numerous multi-scale interactions and adjustments that induce regional differences.

6.5 Paleoclimate

The sensitivity of global-mean temperature to Earth's orbital variations and/or CO₂ natural changes might be considered an analogue of the warming induced by the artificial CO₂ increase, i.e. the climate sensitivity to past climate change an analogue to the equilibrium climate sensitivity (as defined by *Gregory et al.* [2004]). When imposing such past variations, climate models suggest different responses in the strength of global-mean cooling that may be related to the spread in ECS. For instance, *Hargreaves et al.* [2012] shows that the simulated global-mean cooling during the Last Glacial Maximum (LGM, 19-23 ka before present) is inversely correlated with ECS in CMIP3

441 models. Constraining the LGM cooling from proxy data yields a most likely climate sensitivity
442 around 2.3 K, which is lower than emergent constraints based on the mean state or variability
443 (Table 1). A number of criticisms may arise from this inference, such as the realism of the LGM
444 CMIP simulations, uncertainties underlying proxies used for observational reference, and the use
445 of paleoclimates as a surrogate for global warming (differences in temperature patterns, albedo
446 feedback etc.). These uncertainties may partly explain the frequent weak correlations found between
447 paleoclimate indices and climate projections, and the difficulty in narrowing the spread in models'
448 climate sensitivity estimates from paleoclimate-based emergent constraints [*Schmidt et al.*, 2013;
449 *Harrison et al.*, 2015].

450 **7 Do emergent constraints narrow the spread of climate sensitivity so far?**

451 Table 1 lists 11 emergent constraints that provide best estimates for climate sensitivity using
452 various predictors (without paleoclimate indexes). Here I inquire whether taken all together they
453 reduce the raw model uncertainty (e.g., 3.4 ± 0.8 K for CMIP5 models). For that purpose, I build a
454 normal distribution for each of 11 ECS emergent constraints listed on table 1, with mean value and
455 standard deviation taken from the original studies. These values correspond to moments provided by
456 the authors if available, or estimated from the emergent relationship otherwise (and thus correspond
457 to a raw estimate of the real posterior estimate). I attribute each distribution an equal weight of
458 $1/11$, which assume that emergent constraints are independent with each other and equally valuable.
459 Finally, note that the width to each normal distribution is strongly influenced by uncertainties
460 underlying the statistical inference, which differ across studies, and observation uncertainties, which
461 might be sometimes underestimated [e.g. *Volodin*, 2008]. Figure 3 shows all individual distributions,
462 the prior distribution for CMIP models and the combined posterior distribution. It shows that this
463 posterior distribution is really close to the prior distributions, yet slightly skewed toward higher
464 ECS values (explained by the majority of emergent constraints that suggest higher-than-average ECS
465 values). However, the disagreement between emergent constraints and their large uncertainties do not
466 significantly narrow the original spread in ECS. This suggests that emergent constraints need to be
467 better assessed through a verification of physical mechanisms explaining the relationship [*Caldwell*
468 *et al.*, 2018; *Hall et al.*, 2019]. This would give the ability to weight each emergent constraint
469 and provide a better posterior distribution allowing to trustingly narrow the spread in future climate
470 changes. Finally, statistical inference and observational uncertainties need to be better informed for
471 cross-validation of posterior estimates.

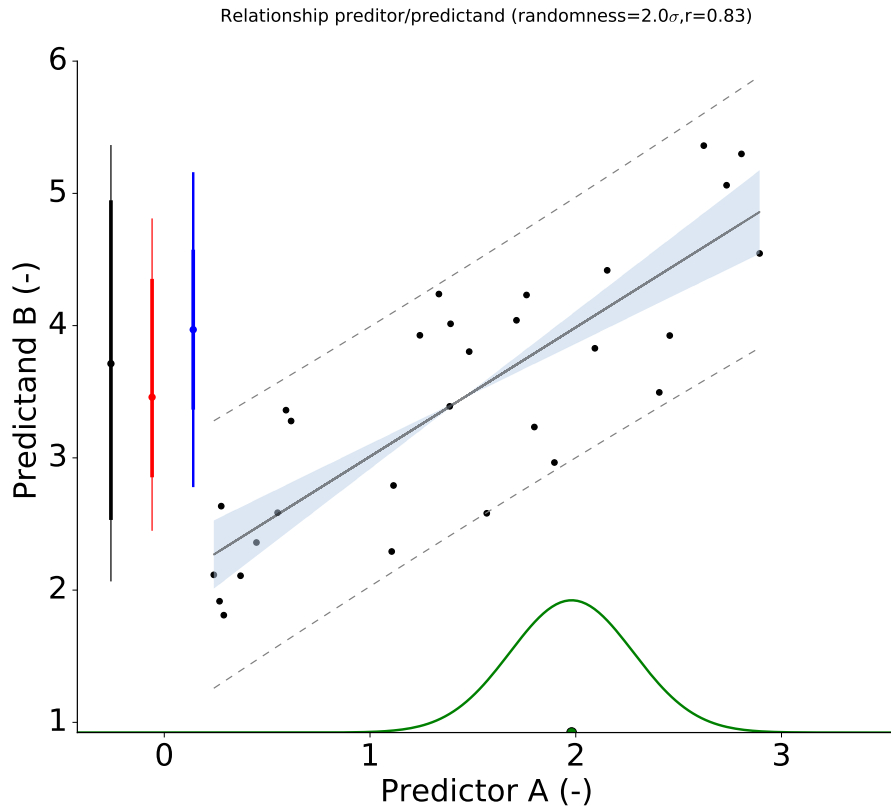
8 Conclusions

This paper presents the concept of emergent constraints, a methodology that aim to narrow uncertainties in climate change projections by identifying a link between them and the inter-model spread in an observable predictor. In the last decade, the number of studies that used this framework grew significantly and provided constraints on various climate projections (an exhaustive list of published emergent constraints is presented on table 1). The majority focused on narrowing uncertainties in equilibrium climate sensitivity, cloud feedback, and carbon cycle feedbacks. Others focused on components of the climate system in relation with changes of the hydrological cycle, the cryosphere, or the dynamical shift of mid-latitude jet, among others. Predictors can be gathered in two main categories: natural variations of the variable of interest with temperature variability or a mean feature of the climate system. This sometimes leads to metrics not directly related to the considered predictand. Physical explanations for emergent constraints are diverse and thus a majority of them remain to be confirmed. Weighting the credibility of emergent constraints would very likely increase the confidence in posterior estimates aimed to narrow the spread in climate projections.

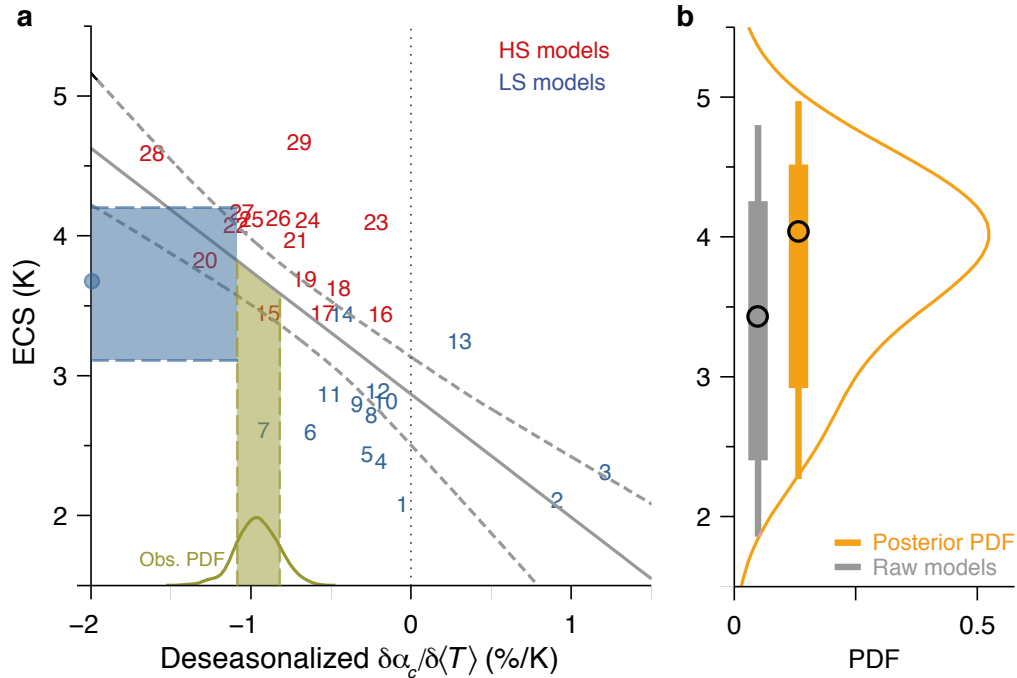
The diversity of emergent constraints highlight the commitment of the climate community to narrowing uncertainties in climate projections. This interest will likely continue to grow since a large number of changes in climate phenomena simulated by models remain uncertain, even when fundamental mechanisms are relatively well understood (e.g., changes in monsoons, heat waves, cyclones). The emergent constraint framework can thus be seen as a new promising way to evaluate climate models [Eyring *et al.*, 2019; Hall *et al.*, 2019], especially with the upcoming CMIP6 project that will very likely boost this enthusiasm. However, this calls for robust statistical inference for providing credible uncertainty reductions. In that purpose, the code used for quantifying inference and uncertainties in Figure 4 with two different methods is shared¹. Quantifying posterior posterior estimates with different frameworks (either from inference or model weighting) allows testing the confidence in predictions. Further improvements would consists in continuing testing difference statistical inference procedures and building multi-predictor weighting method to benefit from the number of proposed emergent constraints .

Beyond the post-facto model evaluation, it will finally be interesting to see whether new climate models take advantage of emergent constraints to improve their simulation of present-day climate and to reduce uncertainties in future projections.

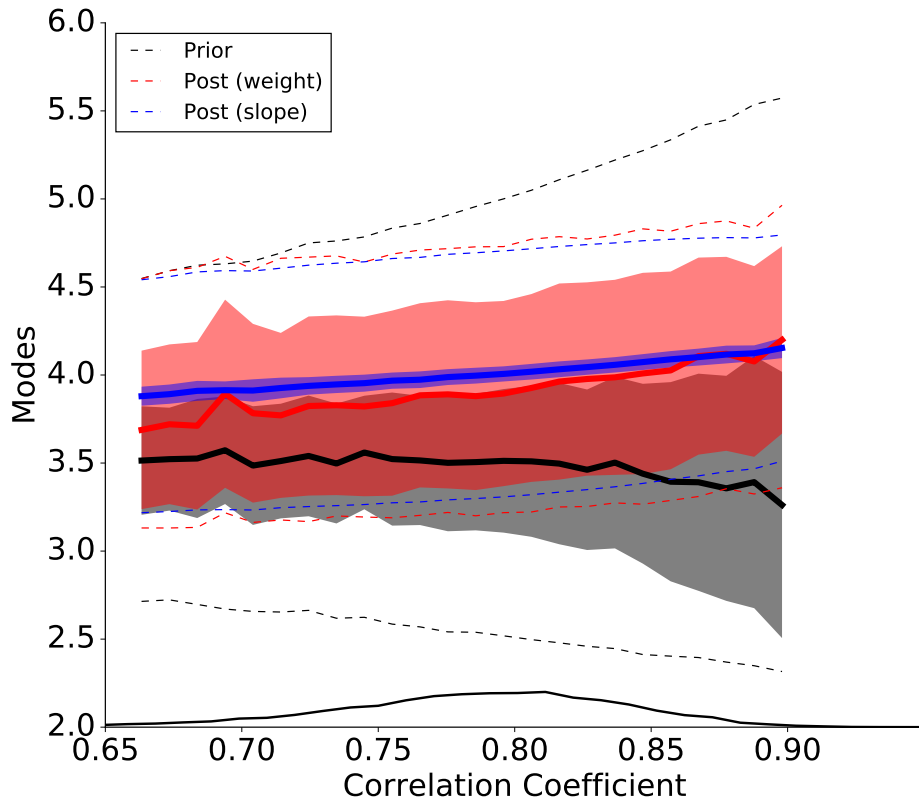
¹ https://github.com/florentbrient/emergent_constraint



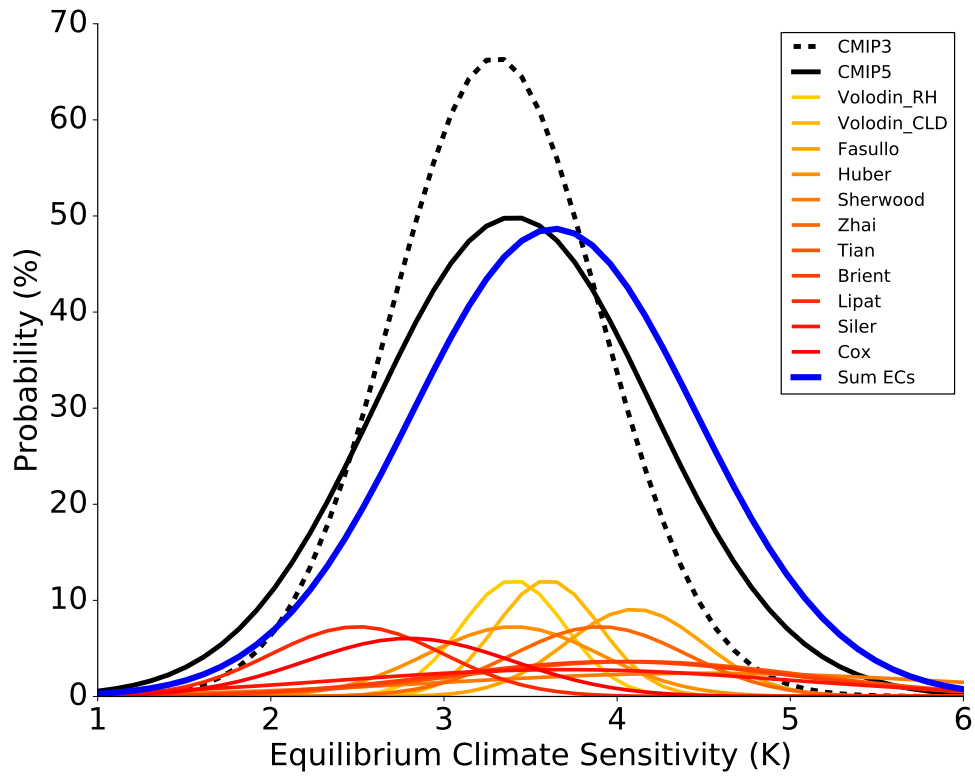
502 **Figure 1.** Idealized relationship between a predictor and a predictand. The 29 models (dots) are associated
 503 with arbitrary values of the predictor A (x here between 0 and 3). The predictand B on the y -axis follows
 504 the idealized relationship ($y' = ax + b$ with $a=1.$ and $b=2.$) plus a random deviation Δ following a normal
 505 distribution with $\sigma=2$ (such as $y = y' + \Delta(y')$). The dashed lines and blue shades represent the 90% prediction
 506 limits and the 90% confidence limits of the slope respectively. The green distribution on the x -axis represents an
 507 idealized observed distribution of the predictor, assuming a normal distribution (here with $\mu=1.98$ and $\sigma=0.3$).
 508 Prior and posterior distributions of the predictand are represented as vertical lines on the left part, with mode
 509 (circle), 66% (thick) and 90% (thin) confidence intervals. Black lines represent the prior distribution, red lines
 510 represent the posterior distribution obtained by a weighted average of the climate models through a Kullback-
 511 Leibler divergence and blue lines are the one inferred using the slope and its uncertainties. In that randomly
 512 generated example, posterior estimates are sensitive to the way inference is computed.



513 **Figure 2.** (a) Scatterplot of ECS vs deseasonalized covariance of marine tropical low-cloud (TLC) reflectance
 514 α_c with surface temperature T in CMIP5 models (numbered in order of increasing ECS). Gray lines represent
 515 a robust regression line (solid), with the 90% confidence interval of the fitted values (dashed) estimated by a
 516 bootstrap procedure. The green line at the lower axis indicates the PDF of the deseasonalized TLC reflectance
 517 variation with surface temperature inferred from observations. The vertical green band indicates the 66% band
 518 of the observations. The blue circle and horizontal band shows the mode and the likely (66%) ECS range inferred
 519 from a linear regression procedure respectively, taking into account uncertainties estimated by bootstrapping
 520 predictions with estimating regression models. (b) Posterior PDF of ECS (orange) obtained by a weighted
 521 average of the climate models, given the observations. The bars with circles represent the mode and confidence
 522 intervals (66% and 90%) implied by the posterior (orange) PDF and the prior (gray) PDF. Adapted from *Brient*
 523 *and Schneider* [2016].



524 **Figure 3.** Relationship between modes and correlation coefficient (r) of 10^4 randomly-generated emergent
 525 constraints, as the example shown on Figure 1. Thick lines, dashed lines and shades represent the average mode,
 526 the average 66% confidence interval and the standard deviation of mode across the set of emergent relationship.
 527 Characteristics of the prior distributions are represented in black color. Posterior estimates using the slope
 528 inference or the weighting averaging are represented in blue and red respectively, using an idealized observed
 529 distribution of the predictor as defined on Figure 1. The probability density function of correlation coefficients
 530 is shown as a thin black line on the x-axis. This figure shows that average modes and confidence intervals
 531 remain independent of the inference method, but the uncertainty of the mode value is larger for the weighting
 532 method.



533 **Figure 4.** Probability density functions (PDFs) of equilibrium climate sensitivity (ECS) from the original
 534 inter-model distribution (CMIP3 and CMIP5 models) and based on posterior distributions derived from 11
 535 emergent constraints listed on table 1. Each emergent constraint PDF is defined as a normal distribution with
 536 mean and standard deviation listed on table 1. The blue line is the ECS distribution covered by all equally-
 537 weighted emergent constraint distributions.

538 **Table 1.** List of 44 published emergent constraints, the predictand they constrain, the original and the constrained ranges. Mean and standard deviations of prior and posterior estimates are listed when available. The
 539 * sign signifies that the moments of the distribution are not directly quantified in the reference paper but derived
 540 from their emergent relationship and the observational constraint, and thus should be understood only as
 541 qualitative assessment.
 542

Reference	Predictand	Original	Constrained
<i>Covey et al.</i> [2000] <i>Volodin</i> [2008] (RH) <i>Volodin</i> [2008] (Cloud) <i>Trenberth and Fasullo</i> [2010] <i>Huber et al.</i> [2011] <i>Fasullo and Trenberth</i> [2012] <i>Sherwood et al.</i> [2014] <i>Su et al.</i> [2014] <i>Zhai et al.</i> [2015] <i>Tian</i> [2015] <i>Brient and Schneider</i> [2016] <i>Lipat et al.</i> [2017] <i>Siler et al.</i> [2018] <i>Cox et al.</i> [2018]	ECS (K)	3.4±0.8 3.3±0.6 3.4±0.8	– 3.4±0.3 3.6±0.3 >4.0 3.4±0.6 4.1±0.4* 4.5±1.5* >3.4 3.9±0.5 4.1±1.0* 4.0±1.0* 2.5±0.5* 3.7±1.3 2.8±0.6
<i>Qu et al.</i> [2013] <i>Gordon and Klein</i> [2014] <i>Brient and Schneider</i> [2016]	Low-cloud amount feedback (%/K) Low-cloud optical depth feedback (K ⁻¹) Low-cloud albedo change (%/K)	-1.0±1.5 0.04±0.03 -0.12±0.28	– – -0.4±0.4*
<i>Siler et al.</i> [2018]	Global cloud feedback (%/K)	0.43±0.30	0.58±0.31
<i>Allen and Ingram</i> [2002] <i>O’Gorman</i> [2012] <i>DeAngelis et al.</i> [2015] <i>Li et al.</i> [2017]	Global-mean precipitation Tropical precipitation extremes (%/K) Clear-sky shortwave absorption (W/m ² /K) Indian Monsoon rainfall changes (%/K)	– 2-23 0.8±0.3 +6.5±5.0	– 6-14 1.0±0.1 +3.5±4.0
<i>Cox et al.</i> [2013] <i>Wang et al.</i> [2014] <i>Wenzel et al.</i> [2014] <i>Hoffman et al.</i> [2014] <i>Wenzel et al.</i> [2016] <i>Kwiatkowski et al.</i> [2017] <i>Winkler et al.</i> [2019]	Tropical land carbon release (GtC/K) CO ₂ concentration in 2100 (ppm) Gross Primary Productivity (%) Tropical ocean primary production (%/K) Gross Primary Production (PgC/yr)	69±39 79±43 49±40 980±161 +34±15 -4.0±2.2 2.1±1.9	53±17 70±45* 44±14 947±35 +37±9 -3.0±1.0 3.4±0.2
<i>Plazzotta et al.</i> [2018]	Global-mean cooling by sulfate (K/W/m ²)	0.54±0.33	0.44±0.24
<i>Hall and Qu</i> [2006] <i>Qu and Hall</i> [2014] <i>Boé et al.</i> [2009] <i>Massonnet et al.</i> [2012] <i>Bracegirdle and Stephenson</i> [2013]	Snow-albedo feedback (%/K) Remaining Arctic sea-ice cover in 2040 (%) Years of summer Arctic ice free Arctic warming (°C)	-0.8±0.3 -0.9±0.3 67±20* [2029-2100+] ~2.78	-1.0±0.1* -1.0±0.2* 37±10* [2041-2060] <2.78
<i>Kidston and Gerber</i> [2010] <i>Simpson and Polvani</i> [2016] <i>Gao et al.</i> [2016] <i>Gao et al.</i> [2016] <i>Douville and Plazzotta</i> [2017] <i>Lin et al.</i> [2017] <i>Donat et al.</i> [2018]	Shift of the South Hemispheric Jet (°) Shift of the North Hemispheric Jet (°) Summer midlatitude soil moisture Summer US temperature changes (°C) Frequency of heat extremes (-)	-1.8±0.7 ~-3 ~0 ~+1.5 – +6.0±0.8 –	-0.9±0.6 ~-0.5* (Winter) ~-2 (Winter) ~-1 (Spring) – +5.2±1.0* –
<i>Hargreaves et al.</i> [2012] <i>Schmidt et al.</i> [2013]	ECS (K)	3.1±0.9 3.3±0.8	2.3±0.9 3.1±0.7

Acknowledgments

This work received funding from grant HIGH-TUNE ANR-16-CE01-0010. I thank Tapio Schneider for the number of discussions we had on this topic, and for sharing his thoughts on statistical inference. I also thank Ross Dixon for interesting discussions and for proofreading the manuscript. Routines for the randomly-generated relationship and the statistical inferences are available on the Github website (https://github.com/florentbrient/emergent_constraint/).

References

- Adam, O., T. Schneider, F. Brient, and T. Bischoff (2016), Relation of the double-ITCZ bias to the atmospheric energy budget in climate models, *Geophys Res Lett*, 43(14), 7670–7677.
- Adam, O., T. Schneider, and F. Brient (2017), Regional and seasonal variations of the double-itcz bias in cmip5 models, *Clim. Dyn.*, pp. 1–17.
- Allen, M. R., and W. J. Ingram (2002), Constraints on future changes in climate and the hydrologic cycle, *Nature*, 419, 224–231.
- Andrews, T., J. M. Gregory, D. Paynter, L. G. Silvers, C. Zhou, T. Mauritsen, M. J. Webb, K. C. Armour, P. M. Forster, and H. Titchner (2018), Accounting for changing temperature patterns increases historical estimates of climate sensitivity, *Geophys Res Lett*, 45(16), 8490–8499.
- Betts, A. K., and Harshvardhan (1987), Thermodynamic constraint on the cloud liquid water feedback in climate models, *J. Geophys. Res.*, 92, 8483–8485.
- Boé, J., A. Hall, and X. Qu (2009), September sea-ice cover in the arctic ocean projected to vanish by 2100, *Nature Geoscience*, 2(5), 341.
- Bony, S., R. Colman, V. Kattsov, R. Allan, C. Bretherton, J.-L. Dufresne, A. Hall, S. Hallegatte, M. Holland, W. Ingram, D. Randall, B. Soden, G. Tselioudis, and M. Webb (2006), How well do we understand and evaluate climate change feedback processes?, *J Clim*, 19(15), 3445–3482.
- Bony, S., G. Bellon, D. Klocke, S. Sherwood, S. Fermepin, and S. Denvil (2013), Robust direct effect of carbon dioxide on tropical circulation and regional precipitation, *Nature Geosciences*, 6(6), 447–451.
- Bony, S., B. Stevens, D. Coppin, T. Becker, K. A. Reed, A. Voigt, and B. Medeiros (2016), Thermodynamic control of anvil cloud amount, *Proc. Nat. Ac. Sci.*, 113(32), 8927–8932.
- Borodina, A., E. M. Fischer, and R. Knutti (2017), Models are likely to underestimate increase in heavy rainfall in the extratropical regions with high rainfall intensity, *Geophys Res Lett*, 44(14), 7401–7409.

- 574 Bracegirdle, T. J., and D. B. Stephenson (2013), On the robustness of emergent constraints used in
575 multimodel climate change projections of arctic warming, *J Clim*, 26(2), 669–678.
- 576 Brient, F., and S. Bony (2013), Interpretation of the positive low-cloud feedback predicted by a
577 climate model under global warming, *Clim. Dyn.*, 40(9-10), 2415–2431.
- 578 Brient, F., and T. Schneider (2016), Constraints on climate sensitivity from space-based measure-
579 ments of low-cloud reflection, *J Clim*, 29(16), 5821–5835.
- 580 Brient, F., T. Schneider, Z. Tan, S. Bony, X. Qu, and A. Hall (2016), Shallowness of tropical low
581 clouds as a predictor of climate models’ response to warming, *Clim. Dyn.*, pp. 1–17.
- 582 Burnham, K. P., and D. R. Anderson (2010), *Model Selection and Multimodel Inference: A Practical*
583 *Information-Theoretic Approach*, 2nd ed., Springer, New York, NY.
- 584 Caldwell, P. M., C. S. Bretherton, M. D. Zelinka, S. A. Klein, B. D. Santer, and B. M. Sanderson
585 (2014), Statistical significance of climate sensitivity predictors obtained by data mining, *Geophys*
586 *Res Lett*, 41(5), 1803–1808.
- 587 Caldwell, P. M., M. D. Zelinka, and S. A. Klein (2018), Evaluating emergent constraints on equilib-
588 rium climate sensitivity, *J Clim*, 31(10), 3921–3942.
- 589 Ceppi, P., and J. M. Gregory (2017), Relationship of tropospheric stability to climate sensitivity and
590 earth’s observed radiation budget, *Proc. Nat. Ac. Sci.*, 114(50), 13,126–13,131.
- 591 Ceppi, P., F. Brient, M. D. Zelinka, and D. L. Hartmann (2017), Cloud feedback mechanisms and
592 their representation in global climate models, *WIREs*.
- 593 Cess, R., M. H. Zhang, W. J. Ingram, G. L. Potter, V. Alekseev, H. W. Barker, E. Cohen-Solal, R. A.
594 Colman, D. A. Dazlich, A. D. D. Genio, M. R. Dix, V. Dymnikov, M. Esch, L. D. Fowler, J. R.
595 Fraser, V. Galin, W. L. Gates, J. J. Hack, J. T. Kiehl, H. L. Treut, K. K.-W. Lo, B. J. McAvaney,
596 V. P. Meleshko, J.-J. Morcrette, D. A. Randall, E. Roeckner, J.-F. Royer, M. E. Schlesinger,
597 P. V. Sporyshev, B. Timbal, K. E. Taylor, E. M. Volodin, W. Wang, and R. T. Wetherald (1996),
598 Cloud feedback in atmospheric general circulation models: An update, *J. Geophys. Res.*, 101,
599 12,791–12,794.
- 600 Cess, R. D., G. Potter, J. Blanchet, G. Boer, A. Del Genio, M. Deque, V. Dymnikov, V. Galin,
601 W. Gates, S. Ghan, et al. (1990), Intercomparison and interpretation of climate feedback processes
602 in 19 atmospheric general circulation models, *J. Geophys. Res.*, 95(16), 601,216.
- 603 Charney, J. G., A. Arakawa, D. J. Baker, B. Bolin, R. E. Dickinson, R. M. Goody, C. E. Leith, H. M.
604 Stommel, and C. I. Wunsch (1979), *Carbon dioxide and climate : a scientific assessment*, 33 pp.,
605 National Academy of Sciences.

- 606 Christensen, J. H., K. K. Kanikicharla, G. Marshall, and J. Turner (2013), Climate phenomena and
607 their relevance for future regional climate change, in *Climate change 2013: the physical science*
608 *basis. Contribution of Working Group I to the Fifth Assessment Report of the Intergovernmental*
609 *Panel on Climate Change*, Cambridge University Press.
- 610 Covey, C., A. Abe-Ouchi, G. Boer, B. Boville, U. Cubasch, L. Fairhead, G. Flato, H. Gordon,
611 E. Guilyardi, X. Jiang, et al. (2000), The seasonal cycle in coupled ocean-atmosphere general
612 circulation models, *Clim. Dyn.*, 16(10-11), 775–787.
- 613 Cox, P. M., D. Pearson, B. B. Booth, P. Friedlingstein, C. Huntingford, C. D. Jones, and C. M. Luke
614 (2013), Sensitivity of tropical carbon to climate change constrained by carbon dioxide variability,
615 *Nature*, 494(7437), 341.
- 616 Cox, P. M., C. Huntingford, and M. S. Williamson (2018), Emergent constraint on equilibrium
617 climate sensitivity from global temperature variability, *Nature*, 553(7688), 319.
- 618 DeAngelis, A., X. Qu, M. Zelinka, and A. Hall (2015), An observational radiative constraint on
619 hydrologic cycle intensification, *Nature*, 528(7581), 249–253.
- 620 Dee, D., S. Uppala, A. Simmons, P. Berrisford, P. Poli, S. Kobayashi, U. Andrae, M. Balmaseda,
621 G. Balsamo, P. Bauer, et al. (2011), The ERA-Interim reanalysis: Configuration and performance
622 of the data assimilation system, *Quart. J. Roy. Meteor. Soc.*, 137(656), 553–597.
- 623 Donat, M. G., A. J. Pitman, and O. Angéilil (2018), Understanding and reducing future uncertainty in
624 midlatitude daily heat extremes via land surface feedback constraints, *Geophys Res Lett*, 45(19),
625 10–627.
- 626 Douville, H., and M. Plazzotta (2017), Midlatitude summer drying: An underestimated threat in
627 cmip5 models?, *Geophys Res Lett*, 44(19), 9967–9975.
- 628 Dufresne, J.-L., and S. Bony (2008), An assessment of the primary sources of spread of global
629 warming estimates from coupled atmosphere-ocean models, *J Clim*, 21(19), 5135–5144.
- 630 Eyring, V., P. M. Cox, G. M. Flato, P. J. Gleckler, G. Abramowitz, P. Caldwell, W. D. Collins, B. K.
631 Gier, A. D. Hall, F. M. Hoffman, et al. (2019), Taking climate model evaluation to the next level,
632 *Nature Climate Change*, p. 1.
- 633 Fasullo, J. T., and K. E. Trenberth (2012), A less cloudy future: The role of subtropical subsidence
634 in climate sensitivity, *Science*, 338(6108), 792–794.
- 635 Flato, G., J. Marotzke, B. Abiodun, P. Braconnot, S. C. Chou, W. Collins, P. Cox, F. Driouech,
636 S. Emori, V. Eyring, et al. (2013), Evaluation of climate models, in *Climate Change 2013: The*
637 *Physical Science Basis. Contribution of Working Group I to the Fifth Assessment Report of the*
638 *Intergovernmental Panel on Climate Change*, pp. 741–866, Cambridge University Press.

- 639 Găinușă-Bogdan, A., P. Braconnot, and J. Servonnat (2015), Using an ensemble data set of turbulent
640 air-sea fluxes to evaluate the ipsl climate model in tropical regions, *J. Geophys. Res.*, *120*(10),
641 4483–4505.
- 642 Gao, Y., J. Lu, and L. R. Leung (2016), Uncertainties in projecting future changes in atmospheric
643 rivers and their impacts on heavy precipitation over europe, *Journal of Climate*, *29*(18), 6711–
644 6726.
- 645 Gordon, N. D., and S. A. Klein (2014), Low-cloud optical depth feedback in climate models, *J.*
646 *Geophys. Res.*, *119*(10), 6052–6065.
- 647 Gregory, J., W. Ingram, M. Palmer, G. Jones, P. Stott, R. Thorpe, J. Lowe, T. Johns, and K. Williams
648 (2004), A new method for diagnosing radiative forcing and climate sensitivity, *Geophys Res Lett*,
649 *31*(3), L03,205.
- 650 Hall, A., and S. Manabe (1999), The role of water vapour feedback in unperturbed climate variability
651 and global warming, *J Clim*, *12*, 2327–2346.
- 652 Hall, A., and X. Qu (2006), Using the present-day seasonal cycle to constrain climate sen-
653 sitivity: A case study of snow albedo feedback, *Geophys Res Lett*, *33*, 1550–1568, doi:
654 10.1029/2005GL025127.
- 655 Hall, A., P. Cox, C. Huntingford, and S. Klein (2019), Progressing emergent constraints on future
656 climate change, *Nat. Clim. Change*, p. 1.
- 657 Hargreaves, J. C., J. D. Annan, M. Yoshimori, and A. Abe-Ouchi (2012), Can the last glacial
658 maximum constrain climate sensitivity?, *Geophys Res Lett*, *39*(24).
- 659 Harrison, S. P., P. Bartlein, K. Izumi, G. Li, J. Annan, J. Hargreaves, P. Braconnot, and M. Kageyama
660 (2015), Evaluation of cmip5 palaeo-simulations to improve climate projections, *Nature Climate*
661 *Change*, *5*(8), 735.
- 662 Hartmann, D. L., and K. Larson (2002), An important constraint on tropical cloud-climate feedback,
663 *Geophys Res Lett*, *29*, 1951–1954.
- 664 Hoffman, F. M., J. T. Randerson, V. K. Arora, Q. Bao, P. Cadule, D. Ji, C. D. Jones, M. Kawamiya,
665 S. Khatiwala, K. Lindsay, et al. (2014), Causes and implications of persistent atmospheric carbon
666 dioxide biases in earth system models, *Journal of Geophysical Research: Biogeosciences*, *119*(2),
667 141–162.
- 668 Huber, M., I. Mahlstein, M. Wild, J. Fasullo, and R. Knutti (2011), Constraints on climate sensitivity
669 from radiation patterns in climate models, *J Clim*, *24*(4), 1034–1052.
- 670 Hwang, Y.-T., and D. M. Frierson (2013), Link between the double-intertropical convergence zone
671 problem and cloud biases over the southern ocean, *Proc. Nat. Ac. Sci.*, *110*(13), 4935–4940.

- 672 Kamae, Y., H. Shiogama, M. Watanabe, T. Ogura, T. Yokohata, and M. Kimoto (2016), Lower-
673 tropospheric mixing as a constraint on cloud feedback in a multiparameter multiphysics ensemble,
674 *J Clim*, 29(17), 6259–6275.
- 675 Kidston, J., and E. Gerber (2010), Intermodel variability of the poleward shift of the austral jet stream
676 in the cmip3 integrations linked to biases in 20th century climatology, *Geophys Res Lett*, 37(9).
- 677 Klein, S. A., and A. Hall (2015), Emergent constraints for cloud feedbacks, *Curr. Clim. Change Rep.*,
678 1(4), 276–287.
- 679 Knutti, R., D. Masson, and A. Gettelman (2013), Climate model genealogy: Generation CMIP5 and
680 how we got there, *Geophys Res Lett*, 40(6), 1194–1199.
- 681 Kwiatkowski, L., L. Bopp, O. Aumont, P. Ciais, P. M. Cox, C. Laufkötter, Y. Li, and R. Sférian
682 (2017), Emergent constraints on projections of declining primary production in the tropical oceans,
683 *Nat. Clim. Change*, 7(5), 355.
- 684 Li, G., S.-P. Xie, C. He, and Z. Chen (2017), Western pacific emergent constraint lowers projected
685 increase in indian summer monsoon rainfall, *Nat. Clim. Change*, 7(10), 708.
- 686 Lin, Y., W. Dong, M. Zhang, Y. Xie, W. Xue, J. Huang, and Y. Luo (2017), Causes of model dry and
687 warm bias over central us and impact on climate projections, *Nature communications*, 8(1), 881.
- 688 Lipat, B. R., G. Tselioudis, K. M. Grise, and L. M. Polvani (2017), C mip5 models’ shortwave cloud
689 radiative response and climate sensitivity linked to the climatological hadley cell extent, *Geophys
690 Res Lett*, 44(11), 5739–5748.
- 691 Masson, D., and R. Knutti (2011), Climate model genealogy, *Geophys Res Lett*, 38(8).
- 692 Massonnet, F., T. Fichefet, H. Goosse, C. M. Bitz, G. Philippon-Berthier, M. M. Holland, and
693 P.-Y. Barriat (2012), Constraining projections of summer arctic sea ice, *The Cryosphere*, 6(6),
694 1383–1394.
- 695 McCoy, D. T., D. L. Hartmann, M. D. Zelinka, P. Ceppi, and D. P. Grosvenor (2015), Mixed-phase
696 cloud physics and southern ocean cloud feedback in climate models, *J. Geophys. Res.*, 120(18),
697 9539–9554.
- 698 Meehl, G. A., G. Boer, C. Covey, M. Latif, and R. Stouffer (2000), The Coupled Model Intercom-
699 parison Project (CMIP), *Bull. Amer. Meteor. Soc.*, 81, 313–318.
- 700 Mitchell, J. F., C. Senior, and W. Ingram (1989), CO₂ and climate: a missing feedback?, *Nature*,
701 341(6238), 132.
- 702 Morice, C. P., J. J. Kennedy, N. A. Rayner, and P. D. Jones (2012), Quantifying uncertainties in global
703 and regional temperature change using an ensemble of observational estimates: The hadcrut4 data
704 set, *J. Geophys. Res.*, 117(D8).

- 705 Myers, T. A., and J. R. Norris (2013), Observational evidence that enhanced subsidence reduces
706 subtropical marine boundary layer cloudiness, *J Clim*, 26(19), 7507–7524.
- 707 Myers, T. A., and J. R. Norris (2015), On the relationships between subtropical clouds and meteo-
708 rology in observations and cmip3 and cmip5 models, *J Clim*, 28(8), 2945–2967.
- 709 O’Gorman, P. A. (2012), Sensitivity of tropical precipitation extremes to climate change, *Nature*
710 *Geoscience*, 5(10), 697–700.
- 711 O’Gorman, P. A., and T. Schneider (2008), The hydrological cycle over a wide range of climates
712 simulated with an idealized GCM, *J Clim*, 21(15), 3815–3832.
- 713 Plazzotta, M., R. Séférian, H. Douville, B. Kravitz, and J. Tjiputra (2018), Land surface cooling
714 induced by sulfate geoengineering constrained by major volcanic eruptions, *Geophys Res Lett*.
- 715 Qu, X., and A. Hall (2014), On the persistent spread in snow-albedo feedback, *Clim. Dyn.*, 42(1-2),
716 69–81.
- 717 Qu, X., A. Hall, S. A. Klein, and P. M. Caldwell (2013), On the spread of changes in marine low
718 cloud cover in climate model simulations of the 21st century, *Clim. Dyn.*, pp. 1–24.
- 719 Qu, X., A. Hall, S. A. Klein, and A. M. DeAngelis (2015), Positive tropical marine low-cloud cover
720 feedback inferred from cloud-controlling factors, *Geophys Res Lett*, 42.
- 721 Qu, X., A. Hall, A. M. DeAngelis, M. D. Zelinka, S. A. Klein, H. Su, B. Tian, and C. Zhai (2018),
722 On the emergent constraints of climate sensitivity, *J Clim*, 31(2), 863–875.
- 723 Rossow, W. B., and R. A. Schiffer (1999), Advances in understanding clouds from ISCCP, *Bull.*
724 *Amer. Meteor. Soc.*, 80, 2261–2287.
- 725 Sanderson, B. M., R. Knutti, and P. Caldwell (2015), A representative democracy to reduce interde-
726 pendency in a multimodel ensemble, *J Clim*, 28(13), 5171–5194.
- 727 Schmidt, G., J. Annan, P. Bartlein, B. Cook, É. Guilyardi, J. Hargreaves, S. Harrison, M. Kageyama,
728 A. LeGrande, B. Konecky, et al. (2013), Using palaeo-climate comparisons to constrain future
729 projections in cmip5, *Climate of the Past*, 10(1), 221–250.
- 730 Seneviratne, S. I., M. G. Donat, A. J. Pitman, R. Knutti, and R. L. Wilby (2016), Allowable co 2
731 emissions based on regional and impact-related climate targets, *Nature*, 529(7587), 477.
- 732 Sherwood, S. C., S. Bony, and J.-L. Dufresne (2014), Spread in model climate sensitivity traced to
733 atmospheric convective mixing, *Nature*, 505(7481), 37–42.
- 734 Siler, N., S. Po-Chedley, and C. S. Bretherton (2018), Variability in modeled cloud feedback tied to
735 differences in the climatological spatial pattern of clouds, *Clim. Dyn.*, 50(3-4), 1209–1220.
- 736 Simpson, I. R., and L. M. Polvani (2016), Revisiting the relationship between jet position, forced
737 response, and annular mode variability in the southern midlatitudes, *Geophys Res Lett*, 43(6),

- 738 2896–2903.
- 739 Stocker, T. F., D. Qin, G.-K. Plattner, M. Tignor, S. K. Allen, J. Boschung, A. Nauels, Y. Xia, V. Bex,
740 P. M. Midgley, et al. (2013), *Climate Change 2013. The Physical Science Basis. Working Group I*
741 *Contribution to the Fifth Assessment Report of the Intergovernmental Panel on Climate Change-*
742 *Abstract for decision-makers, Tech. rep.*, Groupe d’experts intergouvernemental sur l’evolution du
743 climat/Intergovernmental Panel on Climate Change-IPCC, C/O World Meteorological Organiza-
744 tion.
- 745 Su, H., J. H. Jiang, C. Zhai, T. J. Shen, J. D. Neelin, G. L. Stephens, and Y. L. Yung (2014),
746 Weakening and strengthening structures in the hadley circulation change under global warming
747 and implications for cloud response and climate sensitivity, *J. Geophys. Res.*, *119*(10), 5787–5805.
- 748 Tan, I., T. Storelvmo, and M. D. Zelinka (2016), Observational constraints on mixed-phase clouds
749 imply higher climate sensitivity, *Science*, *352*(6282), 224–227.
- 750 Thackeray, C. W., X. Qu, and A. Hall (2018), Why do models produce spread in snow albedo
751 feedback?, *Geophys Res Lett*, *45*(12), 6223–6231.
- 752 Tian, B. (2015), Spread of model climate sensitivity linked to double-intertropical convergence zone
753 bias, *Geophys Res Lett*.
- 754 Trenberth, K. E., and A. Dai (2007), Effects of mount pinatubo volcanic eruption on the hydrological
755 cycle as an analog of geoengineering, *Geophys Res Lett*, *34*(15).
- 756 Trenberth, K. E., and J. T. Fasullo (2010), Simulation of present-day and twenty-first-century energy
757 budgets of the southern oceans, *J Clim*, *23*(2), 440–454.
- 758 Volodin, E. (2008), Relation between temperature sensitivity to doubled carbon dioxide and the
759 distribution of clouds in current climate models, *Izvestiya, Atmospheric and Oceanic Physics*,
760 *44*(3), 288–299.
- 761 Wagman, B. M., and C. S. Jackson (2018), A test of emergent constraints on cloud feedback and
762 climate sensitivity using a calibrated single-model ensemble, *J Clim*, *31*(18), 7515–7532.
- 763 Wang, J., N. Zeng, Y. Liu, and Q. Bao (2014), To what extent can interannual co2 variability
764 constrain carbon cycle sensitivity to climate change in cmip5 earth system models?, *Geophys Res*
765 *Lett*, *41*(10), 3535–3544.
- 766 Wenzel, S., P. M. Cox, V. Eyring, and P. Friedlingstein (2014), Emergent constraints on climate-
767 carbon cycle feedbacks in the cmip5 earth system models, *J. Geophys. Res.*, *119*(5), 794–807.
- 768 Wenzel, S., P. M. Cox, V. Eyring, and P. Friedlingstein (2016), Projected land photosynthesis
769 constrained by changes in the seasonal cycle of atmospheric co 2, *Nature*, *538*(7626), 499.

- 770 Winker, D., J. Pelon, J. Coakley Jr, S. Ackerman, R. Charlson, P. Colarco, P. Flamant, Q. Fu, R. Hoff,
771 C. Kittaka, et al. (2010), The CALIPSO mission: A global 3D view of aerosols and clouds, *Bull.*
772 *Amer. Meteor. Soc.*, *91*(9), 1211–1229.
- 773 Winkler, A. J., R. B. Myneni, G. A. Alexandrov, and V. Brovkin (2019), Earth system models
774 underestimate carbon fixation by plants in the high latitudes, *Nature communications*, *10*(1), 885.
- 775 Zelinka, M., S. Klein, K. Taylor, T. Andrews, M. Webb, J. Gregory, and P. Forster (2013), Contribu-
776 tions of different cloud types to feedbacks and rapid adjustments in cmip5, *J Clim*, *accepted*(2013).
- 777 Zhai, C., J. H. Jiang, and H. Su (2015), Long-term cloud change imprinted in seasonal cloud variation:
778 More evidence of high climate sensitivity, *Geophys Res Lett*, *42*(20), 8729–8737.
- 779 Zhou, C., M. D. Zelinka, A. E. Dessler, and S. A. Klein (2015), The relationship between inter-annual
780 and long-term cloud feedbacks, *Geophys Res Lett*.
- 781 Zhou, C., M. D. Zelinka, and S. A. Klein (2016), Impact of decadal cloud variations on the earth's
782 energy budget, *Nature Geoscience*, *9*(12), 871–874.